Dynamic Behavior of the Geodesic Dome Joints

Nilson Barbieri
Pontifical Catholic University of Paraná, PPGM Federal University of Technology Paraná, UTFPR

Roberto D. Machado
Federal University of Paraná, PPGMNE

Lucas S. V. Barbieri
Federal University of Paraná, PPGMNE

Key F. Lima
Pontifical Catholic University of Paraná, PPGEM

Diego Rossot
Pontifical Catholic University of Paraná, PPGEM

ABSTRACT

In this work the dynamic behavior of a geodesic dome in aluminum alloy is analyzed through numerical models obtained by the Finite Element Method and tests carried out in the laboratory. It was noted that the numerical and experimental results have large differences. Dynamic tests were performed using impulse excitation (impact hammer) and sweep frequency through harmonic excitation (mini-shaker) to identify the natural frequencies of the structure. Using the Theory of Fourier and Wavelet Transform, it was possible to visualize different dynamic behavior of joints. Possible causes for the differences involve the type of joint, the fixing of the elements in the joints, the profile adopted for the elements and boundary conditions for the numerical model.

Keywords
Geodesic dome, vibrations, Wavelet, Fourier transform.

1. INTRODUCTION

Engineers and architects have always a special interest in structures that were able to cover large spans without intermediate columns. In this context, it appears a structure known as a geodesic dome. Following the curved shape of a dome, but constructed from bars, the geodesic dome is a lightweight structure compared with other types. The geodesic domes are structures with a resistance/weight ratio much greater than other types of structure, Ramaswamy (2002) [1]. Currently the use of geodesic domes is associated with large buildings. According to Bysiec (2013) [2] the geodesic domes can be assembled to cover spans over than 300 m without intermediate columns.

The first Geodesic Dome built in history was in Germany in a city named as Jena (Germany) in 1922 . It was a planetary built by Walter Buersfeld for Zeiss industry according Makowski (1981) [3]. However, it is impossible speak on geodesic domes without speak on Fuller. Robert Buckminster Fuller was the bigger sponsor of Geodesic Domes, Kubic (2009)[4]. In his book Synergetics, Explorations in the Geometry of Thinking (1975) [5] wrote about safe energy and develop a world that consume less energy. In this context, he wrote about geodesic domes because it uses less raw material. Fuller classified Geodesic Dome as a special type of Tensegrity Structures, what he considered a bigger group of structures. The name Tensegrity is the contraction between two words "Tensional" and "Integrity". Moreover, Fuller wrote that this kind of structures is continuous different from other structures what he classified how discontinuous. This means that this kind of structure absorb the tension better than other structures. The design of geodesics domes are based on Platonics solids and they are formed by multiple triangles.

Kenner (1976) [6] and Clinton (1965) [7] demonstrated the math to find the coordinates of the nodes that will generate the geodesic dome. They also classified the geodesic domes according to method is used to find the coordinates.

The oil industry has used geodesic dome to cover storage tanks because geodesic domes has helped to avoid evaporation from the storage product and rain water contamination. This happens when geodesic domes are used together with the internal floating roof. The geodesic dome do not need intermediate columns to cover the tank so it allows an increase in efficiency of the internal floating roof. For more details, see Rossot (2014) [8] and Giacomitti et al. (2015) [9].

In this work a physical model based on a real structure was built. The physical model was submitted to dynamic tests. The Frequency Response Function (FRF) and the Wavelet transform were used to investigate dynamic behavior of the joints.

2. PHYSICAL MODEL DESIGN

The physical model was based in a real structure used to cover a gasoline tank with 24 m diameter. The geodesic dome used to cover the gasoline tank is illustrated in Fig. 1. Details about the design as, cross section of the bars, size and coordinates of the nodes, are according Rossot (2014) [8]. In Fig. 2 is shown the pieces that were used to set the physical model. In Fig. 3a is illustrated the physical model already built. Figure 3b shows a detail of a node. Since the aim of this paper is to study the structure of the geodesic dome and the panels used to cover the real geodesic dome are very thin, they was not erected on the physical model.

Fig 1: Geodesic dome used to cover a tank with 24 m diameter.

The structure is composed of 51 beams and 130 joints, Fig. 4. The beams (L profile) were divided into 15 types (B1 to B15) varying according to the length, Table 1. Note that the structure pattern is repeatable at every 72 ° and the bars were considered fixed in the dome border as show the Fig. 5, (see green dots).

Fig 2: Demonstration of the scale of the model.

(a)

(b)

Fig 3: Real model finished.
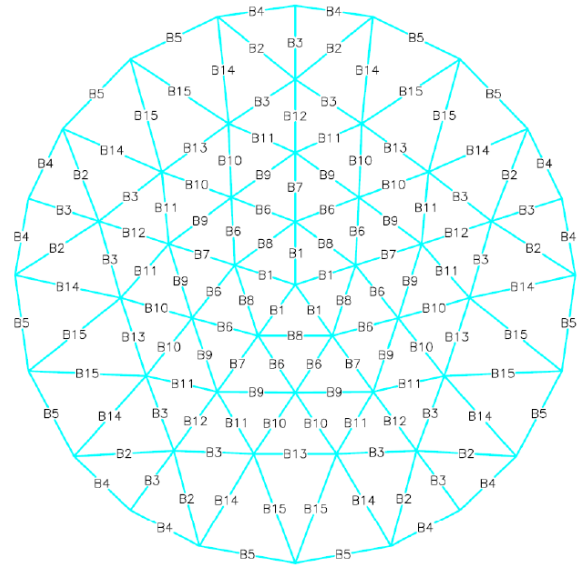
Fig 4: Representation of the beams in the structure.
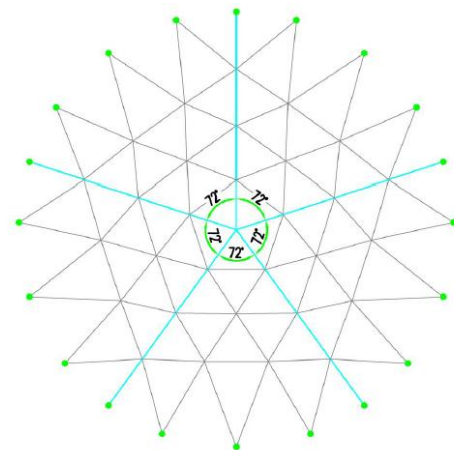
Fig 5: Model symmetry.

Table 1. Size and number of beams in the structure.

Beam	Length (mm)	Quantity
B1	227.93	5
B2	377.80	10
B3	290.75	15
B4	281.14	10
B5	349.40	10
B6	246.44	10
B7	253.51	5
B8	267.58	5
B9	281.40	10
B10	272.90	10
B11	264.30	10
B12	275.58	5
B13	296.19	5
B14	418,80	10
B15	450.82	10

3. DYNAMIC TESTS AND RESULTS

Dynamic test were performed in the laboratory to obtain the modal parameters. The first dynamic tests were carried out using an impact hammer for the system excitation and vibratory data were obtained from six accelerometers placed on the structure, Fig. 6. The specification of the impact

hammer and accelerometers are shown in Table 2.

Fig 6: Impulsive test using impact hammer.

Table 2: Transducers.

Item	Description	Model	Sensibility
1	Impact hummer	086C03-PCB	2.13 mV/N
2	Accelometer	333B-PCB	107.9 mV/g
3	Accelometer	333B-PCB	109.2 mV/g
4	Accelometer	333B-PCB	111.8 mV/g
5	Accelometer	333B-PCB	111.5 mV/g
6	Accelometer	333B-PCB	101.1 mV/g
7	Accelometer	333B-PCB	109.9 mV/g

The main idea this paper is to identify union joints with inadequate structural behavior. The FRF is obtained by correlation between the signal measured by the accelerometer and the impulse signal provided by the impact hammer. The FRFs are obtained as follows: an impulsive force is applied in the point P1 and the accelerations are evaluated at the points A1, A2, A3, A4, A4 and A6, Fig 7. This force is applied 4 times at the same point in order to evaluate the average behavior in accelerometers, Fig. 8 and 9. This procedure is repeated 4 times with the application of impulsive forces at the points P2 to P5. Then, the accelerometers are moved to the positions A1, B2, B3, B4, B5 and B6 and repeats the measurement procedure. The last 6 FRFs are obtained with accelerometers in the positions A1, C2, C3, C4, C5 and C6. Thus, are obtained 18 FRFs. From these signals, a normalized signal is obtained as a function of excitation force. The normalized signal called IFRFs is the inverse of FRFs (Newland, 1996) [10]. The wavelet transform is applied to the signals of IFRF. The purpose of this operation is locate regions of concentration of energy that are related to system resonance frequencies. Through a scan of the signals measured at joints it is possible to identify dynamic behaviors which are not identified in the computational results.

This parameter is the most used for modal identification of structures. Through the analysis of the curves it is possible to identify energy concentration regions associated with the natural frequencies of the system. In a further analysis, the inverse of the FRF signals were converted for the time domain to the use of wavelet theory. The goal was to identify energy concentration regions using vibration signals at the joints. Figure 10 shows the FRF curve of one accelerometer and Fig. 11 the correspondent IFRF four curves (512 points each) of the signal starting with the maximum amplitudes of the four regions shown in Fig. 9. It can be noted in Fig. 10 that there is a region of energy concentration near to frequency band of 30 Hz. This frequency of resonance is not present in the numerical results, where the first natural frequency is around 190 Hz, Table 3. The numerical analysis was performed using the Finite Element Method (FEM). In this work, the FEM was

applied through the software Abacus CAE version 6.14-2 and the geodesic dome was modeled using 3D deformable elements.
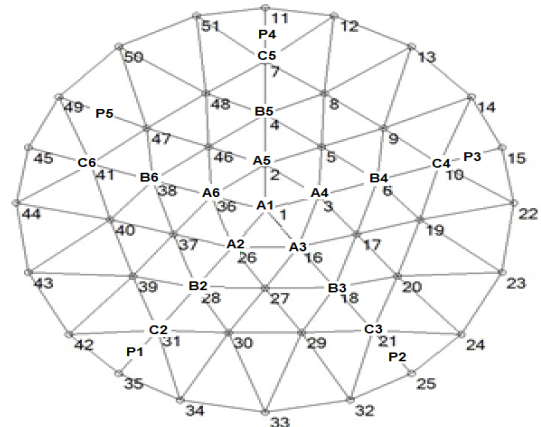
Fig. 7: Acelerometer position.
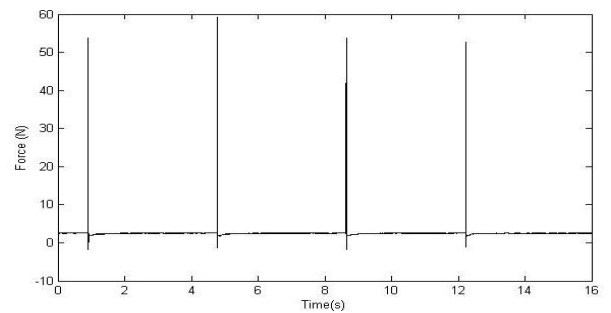
Fig 8: Impulsive force.
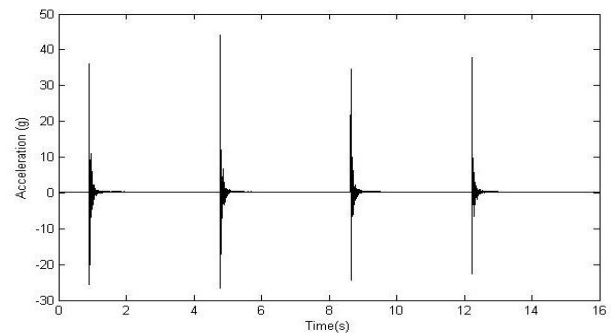
Fig 9: Acceleration signal.
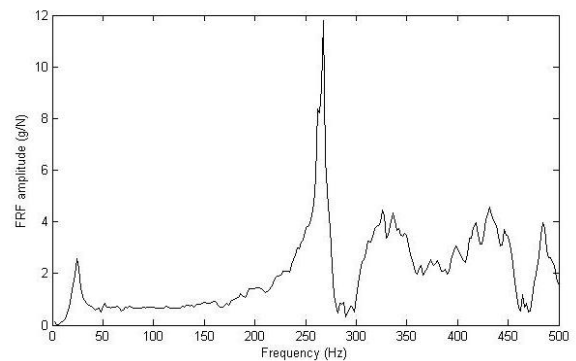
Fig 10: FRF curve.
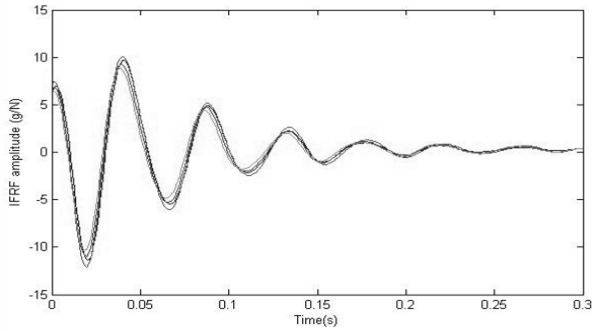
Fig 11: IFRF curve.

Table 3: Ressonance Frequencies.

Mode Number	Frequency [Hz]	Mode Number	Frequency [Hz]
1	186,01	17	220,44
2	186,52	18	221,06
3	187,82	19	222,21
4	193,77	20	223,67
5	193,78	21	225,98
6	193,88	22	227,57
7	197,18	23	228,81
8	197,93	24	229,99
9	202,82	25	230,08
10	205,00	26	235,79
11	205,66	27	239,69
12	206,75	28	241,23
13	210,98	29	243,57
14	213,92	30	245,12
15	216,61	31	248,00
16	218,11	32	252,74

The wavelet transform allows the signal decomposition as a function of time (by translation) and in scale (by dilation or contraction) instead analysis in time and frequency domain as in the case of Fourier Transforms. The time-scale analysis enables detail locally, the information on a sign. Moreover, do not require for the representation of a function, a large amount of coefficients, as is the case of the Fourier Transform. A detailed description of the wavelet transform can be found at Daubechies (1999) [11], Rucka and Wilde (2006) [12] and Lima et al., (2015) [13]. Qin et al., 2015[14]:

The Continuous Wavelet Transform (CWT) is defined as follows:

$$C(a,b) = \int_{-\infty}^{+\infty} f(t)\psi_{a,b}(t)dt$$

(1)

where

$$\psi_{a,b}(t) = a^{1/2}\psi\left(\frac{t-b}{a}\right)$$ (2)

$\psi_{a,b}(t)$ is a window function called the mother wavelet, where a is a scale and b is a translation. An energy index based on (2) was used to analyze de dynamic behavior of the joints. In this case, the analyzed signal was the inverse of the FRF. Figure 12 shows two different curves of energy for two different joints (symmetrical in the model). The lines black and blue represent de Energy index for two signals.
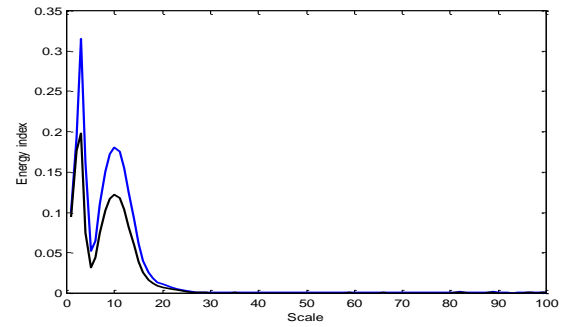
(a)
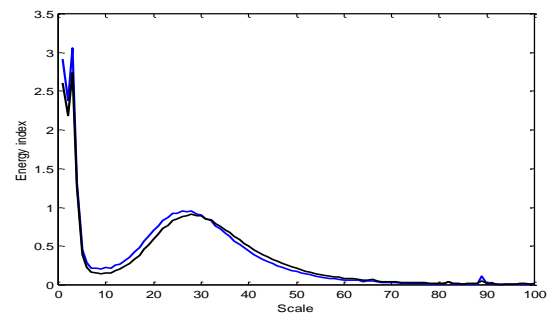
(b)

Fig. 11: Energy curves of two different joints using wavelet transform.

It is evident from the figures that there are large differences in signal behavior in the joints. These energy concentration regions are related to different resonance frequencies of the system.

4. CONCLUSIONS

Dynamic tests using force impulsive was performed. The signals obtained from accelerometers and impedance hummer were handled in Matlab to obtain the curves of Function Frequency Response. All curves were evidenced energy concentration regions to low frequencies: 100 Hz, which corresponds to a value of 10 on the scale of the Fig 11a and 25 Hz, which corresponds to a value of 30 on the scale of the Fig 11b. These frequencies were not contained in the numerical results (see Table 3).

Several factors may have influenced this difference in numeric and experimental values of the natural frequencies. These factors may be related to the way of fixing elements (circular piece and screws that may have gaps); the type of element used (L beam) that for fixing it was necessary to decrease the contact area; the properties of the material (aluminum alloy); the boundary conditions used in the numerical model (the elements of the ends are fixed on a circular structure that was not considered in the numerical model).

5. REFERENCES

[1] Ramaswamy G. S., 2002. Analysis, design and construction of steel space frames. Londres: Thomas Telford.

[2] Bysiec D., 2011. The Investigation of Stability of Double-Layer Octahedron-Based Geodesic Domes. Structure Environment, 3 (3), 30-41.

[3] Makowski, Z. S., 1981. Analysis, Design and Construction of Double-Layer Grids. CRC Press.

[4] Kubic, M., 2009. Structural Analysis of Geodesic Domes. Durham University School of Engineering. Final Year Project.

[5] Fuller, R. B., 1975. Synergetics, explorations in the geometry of thinking. Macmillan Publishing, USA.

[6] Kenner, H., 1976. Geodesic Math and how to use it. California, CA, USA: University of California Press.

[7] Clinton J. Structural Design Concepts for future Space Missions, Progress Report – NASA REPORT, 1965.

[8] Rossot, D., 2014. Domos Geodésicos - Abordagem Numérica e Experimental em um Modelo Físico. Master Dissertation. Pontificia Universidade Católica do Paraná.

[9] Giacomitti, M. R., Machado, R. D., Abdalla, J. E., 2015 Numerical Analysis an Aluminum Geodesic Dome Roof Using the Finite Element Method. |23rd ABCM International Congress of Mechanical Engineering. December 6-11, Brazil.

[10] Newland D. E., 1996. An Introduction to Random Vibrations, Spectral & Wavelet Analysis, Published by Prentice Hall, London.

[11] Daubechies, I., 1999. The Wavelet Transform, Time-Frequency Localization and Signal Analysis, IEEE, Transactions on Information Theory, 36 (5), 961-1005.

[12] Rucka M., Wilde, K., 2006. Application of continuous wavelet transform in vibration based damage detection method for beams and plates. Journal of Sound and Vibration, 297, (3-5), 536-560.

[13] Lima, K. F., Barbieri, N., Barbieri, R., Winniques, L. C., 2015. Young's Modulus and Loss Factor Estimation of Sandwich Beam with Three Optimization Methods by FEM. International Journal of Computer Applications, 128 (3), 35-43.

[14] Qin, J., Sun, P., Walker, J., 2015. A waveform profile-based noise measurement system and methodology for complex noise evaluation. Noise Control Engineering Journal, 63 (9), 563-571.